Analytical and numerical determination of the elastic interaction energy between glissile dislocations and stacking fault tetrahedra in FCC metals

L.Z. Sun [a],[*], N.M. Ghoniem [b], Z.Q. Wang [b]

[a] *Center for Computer-Aided Design and Department of Civil and Environmental Engineering, The University of Iowa, Iowa City, IA 52242-1527, USA*
[b] *Department of Mechanical and Aerospace Engineering, University of California, Los Angeles, CA 90095-1597, USA*

Abstract

Understanding flow localization in materials containing high concentrations of Stacking Fault Tetrahedra (SFT's) depends on delineation of the mechanisms by which they are destroyed as effective dislocation obstacles. The elastic interaction between glissile dislocations and SFT's in FCC metals is examined, both analytically and numerically. Numerical calculations are performed for both full and truncated tetrahedra interacting with edge dislocations, while a new analytical formula is derived for the elastic energy of a full tetrahedron-dislocation system. Calculations confirm that the stress field of glissile dislocations is not sufficient to re-configure SFT's into faulted Frank loops by reverse glide of stair-rod dislocations. This mechanism of SFT destruction by shear unfaulting of Frank loops seems to be unlikely. It is proposed that the destruction of SFT's in irradiated materials is enabled by dislocation drag of interstitial clusters, followed by subsequent recombination and melting of the SFT core. © 2001 Elsevier Science B.V. All rights reserved.

Keywords: Stacking fault tetrahedron; Glissile dislocation; Elastic interaction energy; Dislocation dynamics; FCC metal; Isotropic elastic field

1. Introduction

Lattice defects in metals have a noticeable effect on their bulk mechanical properties. Stacking Fault Tetrahedra (SFT's) are vacancy-type extended defects, which are formed in low stacking fault energy face-centered cubic (FCC) metals and alloys [1,2]. The SFT's can be produced under such diverse experimental conditions as quenching from high temperatures, electron irradiation with high-voltage electron microscope, irradiation with energetic particles, and during heavy plastic deformation [3,4]. Since the first discovery of SFT's in quenched gold foils [5], theoretical investigations of their properties have been extensively pursued [6–9]. However, the main mechanism of SFT destruction by passing glissile dislocations remains unresolved. Recently, the molecular dynamics (MD) method has been used to study the growth and shrinkage of SFT's, and their short-range interaction with point defects [3,10,11]. Such studies give valuable insight into detailed evolution processes of SFT's. Nevertheless, the MD method provides limited information on the long-range elastic interaction between SFT's and other defects such as glissile slip-dislocations. It is also of interest to determine the limitations of elastic theory in the resolution of such short-range dislocation interactions.

Since defects from SFT's are believed to cause irradiation strengthening by their interaction with glissile dislocations [12–14], it is of considerable interest to investigate the interaction process when a glissile dislocation passes close to a stationary SFT. Under irradiation and in quenched metals, "flow channels" are observed to be virtually free of SFT's, while neighboring lattice regions are unaffected. Flow localization thus appears to be controlled by the ability of glissile dislocations to destroy SFT's. The purpose of this work is to elucidate the mechanisms of SFT destruction as a result of its interaction with glissile dislocations. The elastic interaction energy between undissociated glissile dislocations and SFT's is analytically determined. A numerical quadrature procedure is implemented to evaluate line integrals for elastic energy of full or truncated SFT's, and to examine the interactions of dissociated near-by glissile dislocations with SFT's. Viability of various possible mechanisms for destruction of SFT's is discussed. The present computations are carried out on the basis of the isotropic linear theory of elasticity.

2. Analytical and numerical formulas for the elastic energy

2.1. Analytical procedures

For FCC crystals as shown in Fig. 1, the glissile dislocation EF is assumed to have a Burgers vector $a/2[\bar{1}\,0\,1]$,

---

* Corresponding author. Fax: +1-319-335-5660.
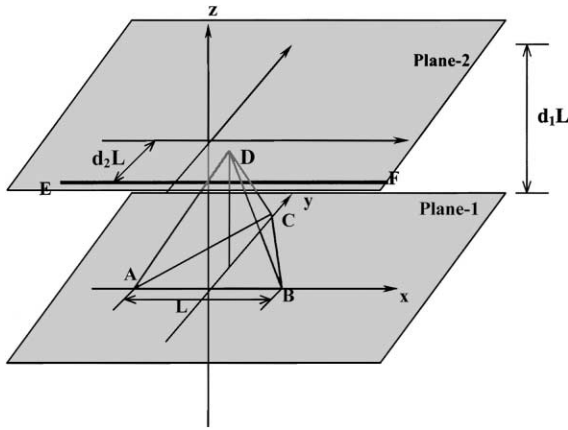*E-mail address:* lizhi-sun@uiowa.edu (L.Z. Sun).

Fig. 1. Local coordinate system for the SFT and the glissile dislocation.

where (a) is the lattice constant, and is mobile on $\{1\,1\,1\}$ planes. The stacking fault tetrahedron ABCD is composed of four triangular faces of ABC, ABD, BCD, and ACD, all of which are within the $\{1\,1\,1\}$ family of planes. In addition, there are a total of six straight dislocation segments, each of which is a stair-rod dislocation with a Burgers vector parallel to the opposite side of the SFT [8]. The elastic interaction energy of a glissile dislocation and an SFT is determined as the sum of the interaction energies between the glissile dislocation and each individual stair-rod dislocation segment.

For simplicity, a local coordinate system (x, y, z) is used to derive the analytical expression for the interaction energy, as shown in Fig. 1. The glissile dislocation is represented by an infinite straight line EF ($y = -d_2L$, $z = d_1L$) in Plane 2 with L as the length of tetrahedron edge. The local Burgers vector of an undissociated glissile dislocation is $\vec{b}_1 = a(-\sqrt{2}/4, \sqrt{6}/4, 0)$. The line representation of stair-rod dislocations and their corresponding Burgers vectors are taken from [1]. The interaction energy between the glissile dislocation and each dislocation segment of the SFT is first calculated from Blin's formula [15,16]. After cumbersome but straightforward calculation of each interaction energy of the infinite dislocation and dislocation segments of the SFT, the total interaction energy E_{int} of the infinite glissile dislocation and the SFT is expressed as

$$
\begin{aligned}
\frac{E_{\text{int}}}{\mu b_1 b_2 L/\pi} \\
= \frac{1}{12(1-\nu)}\left(-1 + \frac{12d_1^2 - 12\sqrt{2}d_1 d_2 + 9d_2^2}{4(d_1^2 + d_2^2)}\right) \\
+ \left[\frac{1}{8(1-\nu)} + \frac{\sqrt{6}}{18}\left(1 - \frac{13}{3(1-\nu)}\right)d_1 \right. \\
\left. + \frac{2\sqrt{3}}{9}\left(1 - \frac{4}{3(1-\nu)}\right)d_2\right]\ln(d_1^2 + d_2^2)
\end{aligned}
$$

$$
\begin{aligned}
+ \left[\frac{1}{4}\left(-1 + \frac{5}{4(1-\nu)}\right) + \frac{\sqrt{6}}{12}d_1 + \frac{\sqrt{3}}{24} \right. \\
\left. \times \left(-4 + \frac{1}{1-\nu}\right)d_2\right]\ln\left[d_1^2 + \left(\frac{\sqrt{3}}{2} + d_2\right)^2\right] \\
+ \left[\frac{1}{4}\left(1 - \frac{7}{4(1-\nu)}\right) + \frac{\sqrt{6}}{36}\left(-5 + \frac{26}{3(1-\nu)}\right)d_1 \right. \\
\left. + \frac{\sqrt{3}}{72}\left(-4 + \frac{55}{3(1-\nu)}\right)d_2\right]\ln\left[\left(\frac{\sqrt{6}}{3} - d_1\right)^2 \right. \\
\left. + \left(\frac{\sqrt{3}}{6} + d_2\right)^2\right] + \frac{\sqrt{3}}{2}\left(-1 + \frac{4}{3(1-\nu)}\right)d_1 \\
\times \arctan\frac{\sqrt{3}d_1}{2d_1^2 + d_2^2 + \sqrt{3}d_2} \\
+ \frac{\sqrt{3}}{18}\left(1 - \frac{2}{3(1-\nu)}\right)(d_1 + 2\sqrt{2}d_2) \\
\times \arctan\frac{\sqrt{3}d_1 + 2\sqrt{6}d_2}{6d_1^2 + 6d_2^2 - 2\sqrt{6}d_1 + \sqrt{3}d_2} \\
+ \frac{\sqrt{3}}{12}\left(1 - \frac{1}{1-\nu}\right)(\sqrt{6} - 2d_1 + 2\sqrt{2}d_2) \\
\times \arctan\frac{-4\sqrt{3}d_1 + 4\sqrt{6}d_2 + 6\sqrt{2}}{12d_1^2 + 12d_2^2 - 4\sqrt{6}d_1 + 8\sqrt{3}d_2 + 3}
\end{aligned} \tag{1}
$$

where b_1 and b_2 are the Burgers vector norms of the glissile dislocation and dislocation segments of the SFT, respectively. Thus, the elastic interaction energy of a glissile dislocation and an SFT is explicitly expressed in terms of the climb and glide distances d_1 and d_2 of the dislocation EF.

2.2. Numerical procedures

To calculate the interaction and self-energy of dislocation loops, we derived compact vector forms for the elastic field variables as functions of convenient parameters that describe the shape of dislocation segments. Each curved dislocation segment is represented in a general parametric form, and the field variables are obtained by numerical quadrature integration with respect to a shape parameter [17]. The displacement vector, strain and stress tensors as well as the self and mutual interaction energies are all expressed in terms of three vectors: the unit tangent $(\vec{t})$, the unit radius $(\vec{e})$ and the Burgers vector $(\vec{b})$. The resulting differential vector and tensor equations, which are composed on of various vector products, can be readily integrated to obtain the total field of closed dislocation loops. The following equation for the interaction energy of two dislocation loops is numerically
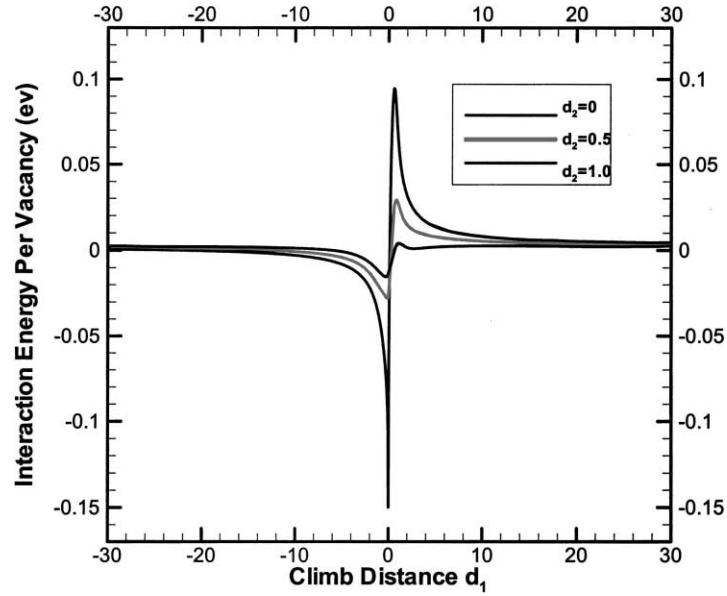
Fig. 2. Change in energy per vacancy in the SFT as a function of the climb distance d_1 in units of L. Negative values indicate reduction in the vacancy formation energy.

integrated

$$\frac{\mathrm{d}^2 E_I}{\mathrm{d}w_1\,\mathrm{d}w_2} = -\frac{\mu T_1 T_2}{8\pi R}\left[2(\vec{b}_1\cdot\vec{t}_1)(\vec{b}_2\cdot\vec{t}_2) - \left(\frac{2}{1-\nu}\right)\right.$$
$$\times(\vec{b}_1\cdot\vec{b}_2)(\vec{t}_1\cdot\vec{t}_2) + \left(\frac{4\nu}{1-\nu}\right)(\vec{b}_1\cdot\vec{t}_2)(\vec{b}_2\cdot\vec{t}_1)$$
$$\left.- \left(\frac{2}{1-\nu}\right)(\vec{t}_1\cdot\vec{t}_2)(\vec{b}_1\cdot\vec{e})(\vec{b}_2\cdot\vec{e})\right] \quad (2)$$

The self-energy of a single dislocation loop is obtained by

setting $\vec{b}_1 = \vec{b}_2 = \vec{b}$ and dividing Eq. (2) by 2, i.e.

$$\frac{\mathrm{d}^2 E_S}{\mathrm{d}w_1\,\mathrm{d}w_2} = -\frac{\mu T_1 T_2}{8\pi R(1-\nu)}\{(1+\nu)(\vec{b}\cdot\vec{t}_1)(\vec{b}\cdot\vec{t}_2)$$
$$-[b^2 + (\vec{b}\cdot\vec{e})^2](\vec{t}_1\cdot\vec{t}_2)\} \quad (3)$$

In the equations, we have defined

$$\vec{T} = \frac{\mathrm{d}\vec{l}}{\mathrm{d}w}, \qquad T = |\vec{T}|, \qquad \vec{t} = \frac{\vec{T}}{T}, \qquad \vec{e} = \frac{\vec{R}}{R} \quad (4)$$
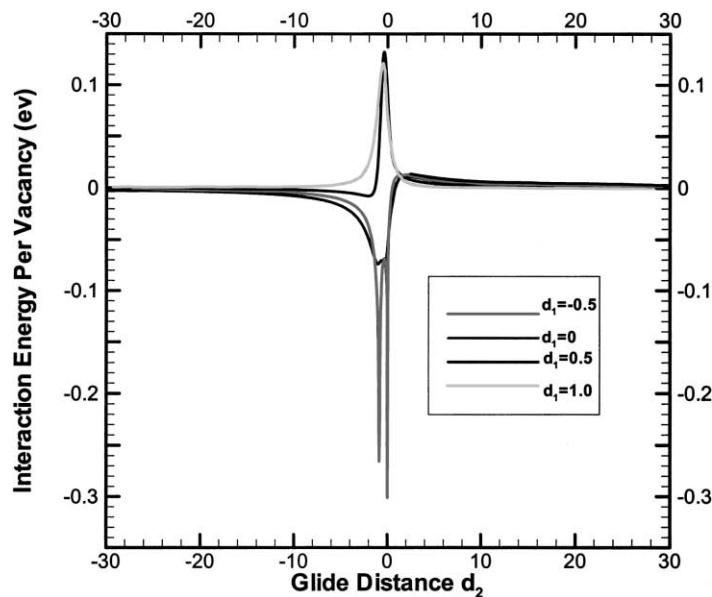

Fig. 3. Change in energy per vacancy in the SFT as a function of the glide distance d_2 in units of L. Maximum interaction energy occurs when the dislocation is inside the SFT ($d_1 = 0$).

Note that these forms are different from Blin's formula, because they contain only vector products with no second-order tensor components. The results agree with Blin's formula only for closed loops, as already noted by deWit [8].

3. Results

Consider Cu as a typical example of an FCC material, the shear modulus μ and Poisson's ratio ν are chosen as 50 GPa and 0.31, respectively. The edge length L of an SFT is taken as 2.5 nm [18]. The Burgers vector norms of glissile dislocation and SFT dislocation segments are $\sqrt{2}/2a$ and $\sqrt{2}/6a$, respectively, where $a = 0.36$ nm represents the lattice constant of Cu. From Eq. (1), the interaction energy E_{int} is calculated as a function of the distance d_1 and d_2, as shown in Figs. 2 and 3. The energy parameters is expressed in the convenient unit of (eV/vacancy) in the SFT, and the glissile dislocation is assumed to be undissociated for simplicity of analytical calculations. It is noted that the interaction energy decays slowly as the glissile dislocation moves away from the SFT. As can be seen from Fig. 2, the interaction energy is negative when the SFT is on the
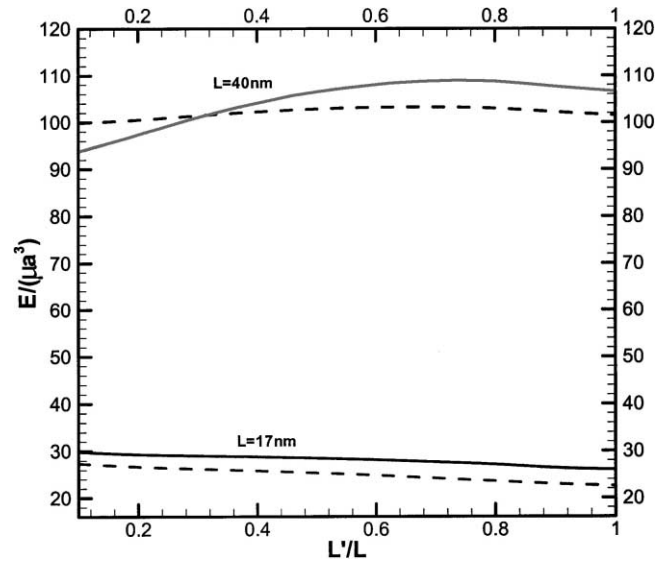

Fig. 4. Self-energy of truncated SFT for Au as a function of the reduced truncated height (L'/L). The solid lines represent the analytical results [7], while the dashed lines are to present numerical calculations (128 quadrature points).
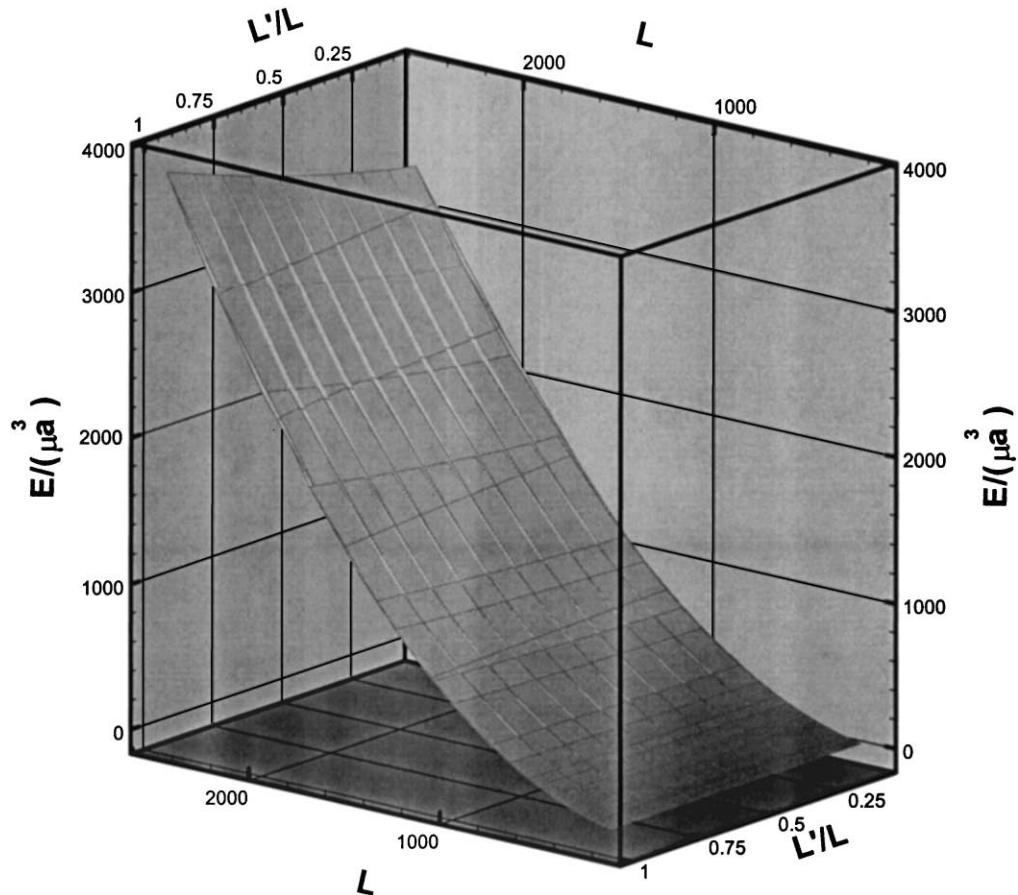

Fig. 5. 3D display of SFT self-energy energy dependence on its size (L, Angstroms) and its truncated height L' (64 quadrature points).
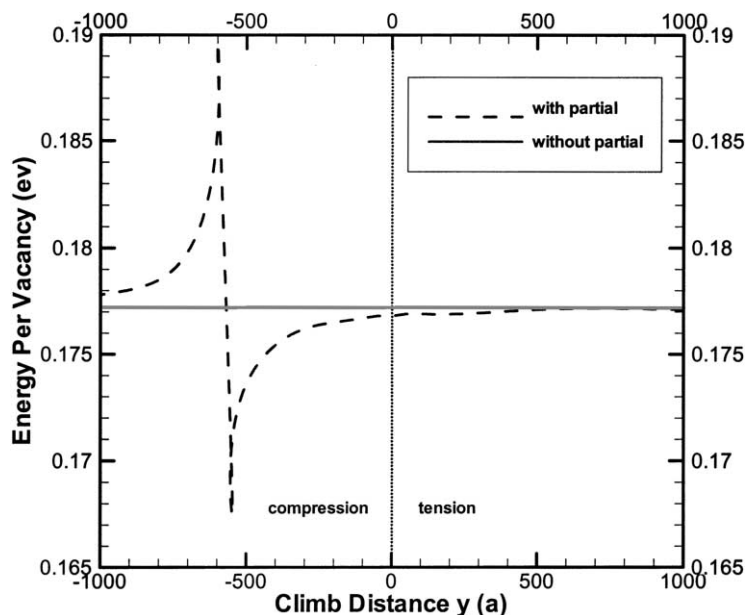
Fig. 6. Change in energy per vacancy for the SFT as a result of its interaction with split partial dislocations in Au (the size of the tetrahedral is $L = 17$ nm and the length of partial dislocations is 950 nm). The dotted line represents the position of glide plane.

compressive side of the edge dislocation (i.e. for negative d_1). This negative interaction becomes significant with the glissile dislocation is closest to the SFT. The strong interaction is also shown in Fig. 3, where the glissile dislocation moves horizontally towards the SFT. However, it is shown that the interaction energy does not change sign as the glissile passes by the SFT from the positive to the negative side. If the glissile dislocation glides along the (1 1 1) plane which is above the bottom of SFT, it will feel a strong resistance force (the derivative of this interaction energy), which is maximum when the dislocation is just above (or inside) the SFT. On the other hand, the glissile dislocation will encounter attraction from the SFT if it moves horizontally under its bottom. The present model ignores the deformation of the glissile dislocation line as it approaches the SFT.

Fig. 4 shows the results of numerical integration of the self-energy Eq. (3) for truncated SFT in Au as a function of the reduced truncated height of the SFT. The agreement between the numerical calculations and analytical results is quite good, even though the form of the energy equation is different from Blin's formula used in the analytical calculations. The dependence of the self-energy of perfect and truncated tetrahedra on their size (in Angstroms) is shown in Fig. 5. As already observed by Jossang and Hirth [7], the energy of a perfect tetrahedron is smaller than its truncated counterpart, indicating that its tendency to reconfigure by pulling down the stair-rod dislocations is indeed negligible until it is of unrealistically large size. Experimental observations [18] of irradiated materials show that very small ($L = 2.5$ nm) SFT's are stable.

The possibility of a nearby glissile dislocation providing enough energy to the perfect tetrahedron to assist in its re-

configuration into a Frank loop is examined next. Fig. 6 shows the change in energy per vacancy for the SFT as a result of its interaction with split partial dislocations in Au (the size of the tetrahedron is $L = 17$ nm and the length of partial dislocations is 950 nm). It is observed that the change in the vacancy formation energy due to the contraction of the elastic field surrounding the SFT is 0.176 eV in Au for the 17 nm tetrahedron. Such a change in the vacancy formation energy is indeed small, and would not by itself lead to significant vacancy emission rate at room temperature. The influence of a nearby glissile dislocation on the change in vacancy formation energy is also shown in Fig. 6. It is clear that the stress field of a split dislocation with two partials would not lead to a great modification of the energy, which is, at most, 0.19 eV. Smaller size tetrahedra are found to be more sensitive to the stress field of nearby glissile dislocations.

4. Discussion and conclusions

The current results indicate that the contribution of the stress field of glissile dislocations to the total elastic energy (self and interaction) is small. The change in energy as a result of glissile dislocations passing by tetrahedra does not appear to be sufficiently large to reconfigure it into a faulted Frank loop. Destruction of the tetrahedron by this mechanism appears to be unlikely, since stable tetrahedra of very small size are experimentally observed. Contraction of the elastic field around the tetrahedron can change the vacancy formation energy, and hence may lead to accelerated vacancy emission and dissolution of the tetrahedron. However,

this mechanism may not be totally responsible for the removal of SFT's by glissile dislocations, unless some local heating is also present.

Assuming that dislocations can drag interstitial atoms or interstitial clusters as they approach stationary dislocations, simple calculations for the adiabatic temperature rise within the tetrahedron volume when it is fully recombined with interstitials indicate that the local temperature exceeds the melting point. These calculations are based on 5 eV energy release for each recombination event between vacancies and interstitials, and the simple adiabatic results give a temperature rise of ~7500 K within the tetrahedron volume. If only a few interstitials recombine, the local temperature rise will be sufficient to accelerate vacancy emission and absorption into the dislocation core. Thus, if this scenario is plausible, local melting of the tetrahedron will follow, and all of most of its vacancies would be absorbed in the dislocation core, leading to further formation of climb jogs.

In summary, we draw the following conclusions from the present work:

1. The contribution of glissile dislocations to the total elastic energy of nearby SFT's is small, as compared to the SFT self-energy.
2. The mechanism of reverse glide of stair-rod dislocations, assisted by its interaction with partial glissile dislocations seems to be an unlikely explanation for its destruction.
3. The change in the vacancy formation energy within the SFT in only significant for very small size SFT (<3 nm). Vacancy emission followed by pipe diffusion requires local high temperatures.
4. It is suggested that massive recombination of vacancies within the SFT occurs as a result of its interaction with jogged/decorated dislocations. Energy release may provide a sufficient temperature rise for SFT dissolution.

Acknowledgements

References

[1] J.P. Hirth, J. Lothe, Theory of Dislocations, 2nd Edition, Wiley, New York, 1982.
[2] M. Kiritani, Mater. Chem. Phys. 50 (1997) 133.
[3] Y.N. Osetsky, A. Serra, M. Victoria, S.I. Golubov, V. Priego, Philos. Mag. A 79 (1999) 2259.
[4] M. Kiritani, J. Nucl. Mater. 276 (2000) 41.
[5] J. Silcox, P.B. Hirsch, Philos. Mag. 4 (1959) 72.
[6] D. Kuhlmann-Wilsdorf, Acta Metal. 13 (1965) 257.
[7] T. Jossang, J.P. Hirth, Philos. Mag. 13 (1966) 657.
[8] R. de Wit, Phys. Statist. Solidi 20 (1967) 575.
[9] P. Humble, R.L. Segall, A.K. Head, Philos. Mag. 15 (1967) 281.
[10] Y. Shimomura, Mater. Chem. Phys. 50 (1997) 139.
[11] Y.N. Osetsky, A. Serra, M. Victoria, S.I. Golubov, V. Priego, Philos. Mag. A 79 (1999) 2285.
[12] M. Saxlova, Czech. J. Phys. B 19 (1969) 610.
[13] H. Trinkaus, B.N. Singh, A.J.E. Foreman, J Nucl. Mater. 249 (1997) 91.
[14] N.M. Ghoniem, B.N. Singh, L.Z. Sun, T.D. de la Rubia, J. Nucl. Mater. 276 (2000) 176.
[15] J. Blin, Acta Metal. 3 (1955) 199.
[16] L.P. Kubin, J. Kratochvil, Philos. Mag. A 80 (2000) 201.
[17] N.M. Ghoniem, L.Z. Sun, Phys. Rev. B 60 (1) (1999) 128.
[18] B.N. Singh, D.J. Edwards, P. Toft, J. Nucl. Mater., 2000, in press.